***JKPK (JURNAL KIMIA DAN PENDIDIKAN KIMIA)**, Vol. 8, No.1, 2023* *pp. 13-25*
Chemistry Education Study Program, Universitas Sebelas Maret *ISSN 2503-4146*
https://jurnal.uns.ac.id/jkpk *ISSN 2503-4154 (online)*

SYNTHESIS AND PHOTOCATALYTIC ACTIVITY TEST OF Bi-TiO_2 TOWARD HUMIC ACID DEGRADATION UNDER VISIBLE LIGHT IRRADIATION

Efraimi Caroline Dien, Anthoni B. Aritonang* and Gusrizal Gusrizal

Department of Chemistry, Faculty of Mathematics and Natural Sciences, Tanjungpura University, Pontianak, Indonesia
Jl. Prof. Dr. H. Hadari Nawawi, Pontianak, West Kalimantan, Indonesia

* For correspondence purposes, email: anthoni.b.aritonang@chemistry.untan.ac.id

Received: January 14, 2023 Accepted: April 14, 2023 Online Published: April 20, 2023
DOI : 10.20961/jkpk.v8i1.71525

ABSTRACT

Humic acid (HA) in water can harm humans if it is regularly used or consumed. HA causes problems in the water, such as color, taste, and the formation of metal complexes. Therefore, it is necessary to degrade HA to address these problems. In this study, HA degradation was carried out using bismuth-doped TiO_2 (Bi-TiO_2) as a photocatalyst. The effect of Bi-TiO_2 synthesized at various Bi concentrations and calcination temperatures on HA degradation was investigated and compared to pristine TiO_2. Bi-TiO_2 was synthesized via the sol-gel method and characterized using X-Ray Diffraction (XRD), Diffuse Reflectance Spectroscopy UV-Visible (DRS UV-Vis), and Fourrier Transform-Infra Red (FT-IR) Spectroscopy. The XRD analysis showed that the optimum calcination temperature was 500^{o}C, with the highest crystallinity index (62.04%) and smallest crystallite size (11.95 nm). The DRS UV-Vis analysis showed that Bi-TiO_2 1.5% led to the lowest band gap of 1.59 eV (λ = 782.33 nm), indicating that the photocatalyst was active under visible light irradiation. The FT-IR analysis showed an adsorption peak from the Bi-O bond at 802.39 cm^{-1}, which caused a shift in the Ti-O-Ti adsorption peak. The photodegradation test was conducted using a 30 mL volume of HA solution 50 ppm and a 50 mg mass of catalyst. The results showed that Bi-TiO_2 1.5% exhibited the highest efficiency in degrading HA, achieving 68.54% under visible light irradiation for 180 minutes. These results suggest the potential of Bi-TiO_2 as an alternative method for treating HA in peat water using visible light irradiation.

Key word: synthesis, Bi-TiO_2, photocatalysis, degradation, humic acid

INTRODUCTION

Clean water is one of the primary needs of living things, but its availability in nature is increasingly limited, along with high population growth. Industrial development also contributes to surface water pollution, such as organic pollutants and microorganisms, so the surface water quality decreases. In addition, peat water has not been used because it contains high levels of humic acid and vulvic acid, which can be detrimental to health.

Humic acid (HA) is a complex compound having both aromatic and aliphatic components and is commonly found in nature, such as rivers and soil [1]. HA, presence in water and soil causes brownish to blackish colour. In addition, HA may react in the environment with metal, forming metal-humic acid ions [2]. Therefore, water disinfection using chlorine in water

containing HA causes the formation of trihalomethanes (carcinogenic compound) as a disinfecting byproduct that harms humans [3].

Common methods for HA removal in water include coagulation, flocculation, adsorption, and filtration. However, these methods have limitations such as high cost, not being eco-friendly, difficulty in separation, and low efficiency [4]. Amongst these methods, alternative methods, such as photocatalysis, are required to evaluate HA removal in water treatment. The photocatalysis semiconductor method has advantages, such as low production cost, environmentally friendly, and harmless. Photocatalysis has been extensively used for the degradation of organic pollutants because the photogenerated electron-hole pairs induce the formation of hydroxyl radicals (•OH). These •OH will degrade HA producing degraded products, such as CO_2 and H_2O [5].

Titanium dioxide (TiO_2) is a semiconductor material that has been widely applied as a photocatalyst material. However, TiO_2 has a wide band gap value (3.2 eV). The band gap value means that this photocatalyst is only active under UV irradiation as a light source and needs to be modified by doping. TiO_2 doping with metallic elements such as bismuth (Bi) can form impurity levels between valence and conduction bands, causing crystal defects to extend the spectral range to visible light irradiation [6]. In addition, bi as a dopant can inhibit the recombination of electron-hole pairs during photoreaction.

Bi has been reported to have the ability to enhance the photocatalytic activity of TiO_2 under visible light irradiation. Bi-TiO_2 has been synthesised for RhB degradation reaching 85% under visible light irradiation [7]. On the other hand, Bi-TiO_2 has been syntesized for acetaminophen degradation, reaching 98% under visible light irradiation [8].

This study emphasized the synthesis of TiO_2 and Bi-TiO_2 by sol-gel method at various Bi concentrations (0.5%, 1%, and 1.5% (w/v)) to investigate the effect of Bi doping on band gap (Eg) value. This synthesis used titanium tetraisopropoxide (TTiP) as Ti precursor and bismuth nitrate pentahydrate ($Bi(NO_3)_3.5H_2O$) as Bi precursor. Also, this study was undertaken to investigate the effect of various calcination temperatures (400°C, 500°C, and 600°C) of Bi-TiO_2 on XRD patterns, crystallite size, and crystallinity index. As-synthesized Bi-TiO_2 was then characterized using XRD, DRS UV-Vis, and FT-IR to obtain crystal structure, optical properties, and functional groups from as-synthesized Bi-TiO_2. Previous studies showed that Bi could be used to enhance TiO_2 photocatalytic activity under visible light irradiation for the degradation of organic pollutants. This study used various Bi concentrations and calcination temperatures to evaluate its photocatalytic activity on HA degradation under visible light irradiation for HA treatment in peat water.

METHODS

All chemicals used for the present work were of analytical grade. Acetilacetone ($C_5H_8O_2$, 99.9%), ammonium hydroxide (NH_4OH, 25%), bismuth nitrate pentahydrate ($Bi(NO_3)_3.5H_2O$, for analysis), and nitric acid (HNO_3, 65%) were obtained from Merck. Humic acid and titanium tetraisopropoxide ($C_{12}H_{28}O_4Ti$, 97%) were obtained from Sigma-Aldrich. Ethanol (C_2H_5OH, 99.9%) was obtained from Smart-Lab. Distilled water

was used throughout the synthesis and photocatalysis activity test.

Instruments used for characterized samples were Diffuse Reflectance Spectroscopy UV-Visible (DRS UV-Vis), Fourier Transform-Infra Red (FT-IR), Spectrophotometer UV-Visible, and X-Ray Diffraction (XRD). The DRS UV-Vis was recorded on Agilent Cary 60, and $BaSO_4$ was used as a reference for reflectance spectra. The FT-IR was recorded on Shimadzu IR Prestige 21 and was carried out in a wavenumber range of 4000-400 cm^{-1}. The UV-Vis spectrophotometer was recorded on Shimadzu UV-1280 and was carried out using a wavelength range of 200-800 nm. The XRD was recorded on an X'PERT PRO PANanalytic X-ray diffractometer (Philips) using Cu Kα radiation (λ = 1.5406 Å, 30 mA, 40 kV) in the range 2θ of 20-80°.

Synthesis of TiO_2

TiO_2 was synthesized by sol-gel method and shown in Figure 1 [9]. Sol $Ti(OH)_n$ was made by mixing solvent A (acetic acid, distilled water, and ethanol) and solvent B (titanium tetraisopropoxide (TTiP) and ethanol) solutions. 2 mL acetic acid and 2 mL distilled water were dissolved in 26.5 mL ethanol. Then 7.5 mL TTiP was added slowly to 26.5 mL ethanol in a reflux flask. The mixture in the reflux flask was stirred using a magnetic stirrer, and 1 mL acetylacetone was added to the mixture. Afterwards, solution A was added in drops to solution B and stirred at 50-55°C for 2 hours to obtain a homogenous mixture. The obtained mixture was aged at room temperature for ± 1 month until a gel had formed. The obtained gel was dried at 85°C for 2 hours and calcinated at 450°C for 3 hours.

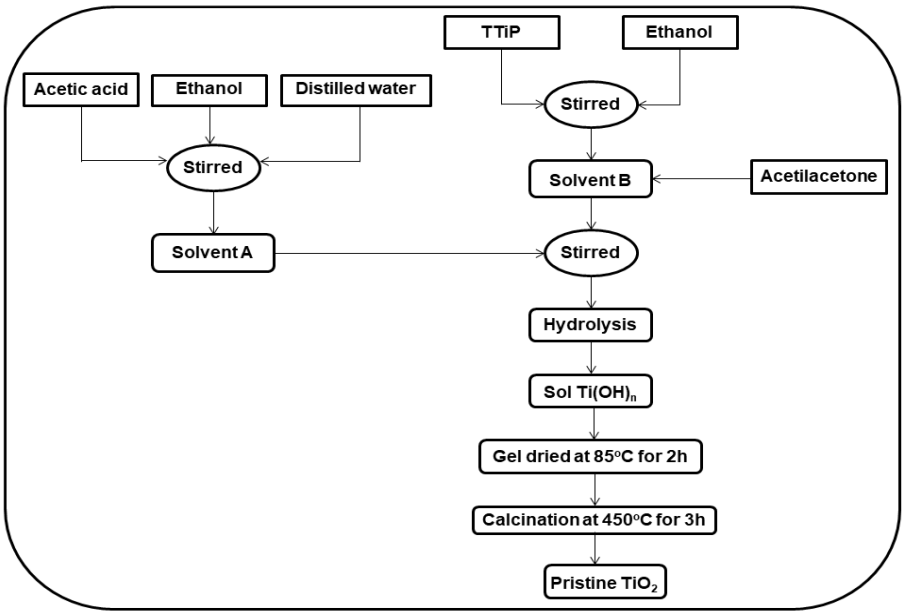

Figure 1. Flowchart for Synthesis of TiO_2

Synthesis of Bi-TiO_2

Bi-TiO_2 was synthesized by the sol-gel method and shown in Figure 2 [10]. Bi-TiO_2 was synthesized using $Bi(NO_3)_3.5H_2O$ by various Bi concentrations (0.5%; 1%; and 1.5% (w/v)). A calculated amount of

$Bi(NO_3)_3.5H_2O$ was dissolved in distilled water by adding a few drops of HNO_3 (qualitative) for better solubility. Following this step, the mixture was in drops to $Ti(OH)_n$ sol in a reflux flask and 4 to 5 drops of NH_4OH were added and stirred for 2 hours using a magnetic stirrer. The obtained mixture was aged at room temperature for 24 hours. The gel was dried at 80°C for 2 hours and calcinated at 400°C, 500°C, and 600°C for 3 hours.

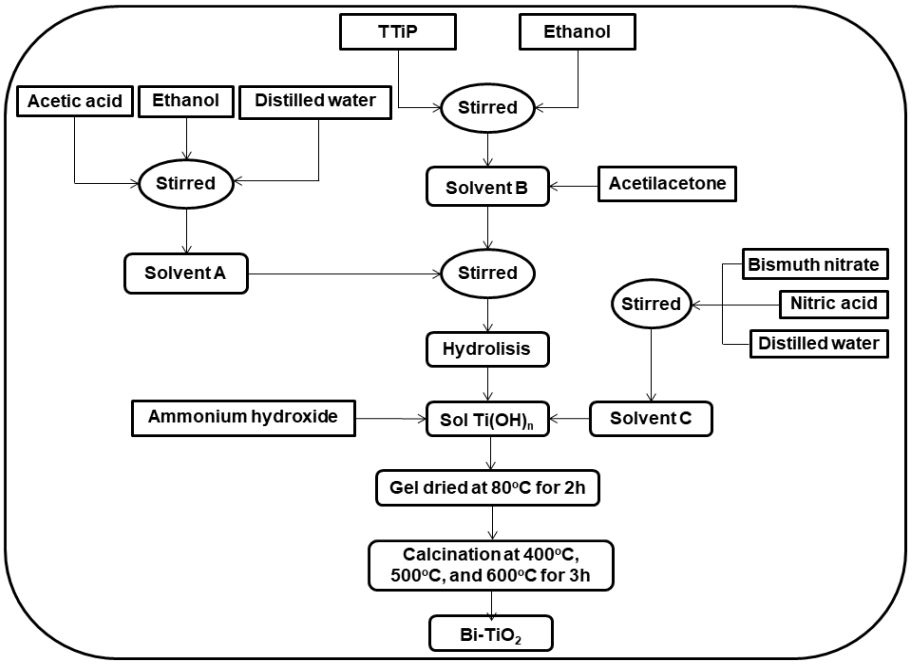

Figure 2. Flowchart for Synthesis Bi-TiO_2

Photocatalytic Activity of Bi-TiO_2 for Humic Acid Degradation

Photocatalytic degradation was performed by the previous modified method reported by [11]. 30 mL HA solution 50 ppm was added to the photoreactor. The solution was added to a 100 mL Pyrex reactor, and irradiation was carried out using a 20-watt LED lamp above the batch photoreactor. Experiments were carried out in batch reactor (40 cm in width and 50 cm in height). The distance between the solution and the visible light source was constant at 15 cm.

50 mg of TiO_2 and Bi-TiO_2 (0.5%; 1%; and 1.5% (w/v)) photocatalyst were added to HA solution. A 20 watt LED lamp (7.1 klx) was the light source. The solution mixture with photocatalyst was stirred and irradiated in the photoreactor for 3 hours. The photocatalytic activity was conducted at approximately 28°C using a circulating air system. The colloidal solution (5 mL) was centrifuged for 5 minutes at 1500 rpm every 20 minutes, and the separated solution was obtained. The remaining HA concentration was measured by UV-Vis spectrophotometer at a maximum absorption wavelength of 254 nm, and distilled water was used as a blank sample. The photodegradation (%) efficiency of HA as a function of time is calculated by the equation :

$$\% = \frac{C_o - C_f}{C_f} \times 100\% \quad (1)$$

Co is the initial concentration of HA (mg/L), and Cf is the HA (mg/L) in a period.

RESULTS AND DISCUSSION

Characterization by XRD, DRS UV-Vis, and FT-IR Analysis

XRD characterization was used to investigate the crystal phase, crystallite size, and crystallinity index of the synthesized pristine TiO_2 and Bi-TiO_2. XRD patterns of pristine TiO_2 and Bi-TiO_2 at different temperatures are shown in Figure 3. Figure 3 shows that different calcination temperatures affected the peaks from sharper, narrower, and higher intensity peaks with increasing temperatures [12, 13]. With increasing calcination temperature, diffraction peaks were steadily sharper and narrower, which attributed to the elimination of grain boundary defects during calcination temperature at 500°C and 600°C [14]. The XRD results exhibit a specific diffraction pattern. The obtained pristine TiO_2 peaks are 25.3°; 37.7°; 48°; 53.9°; 55°; and 62.7° by planes of the anatase phase (JCPDS cards No. 12-1272). These peaks correspond to (101), (004), (200), (105), (211), and (204) crystal planes [15].

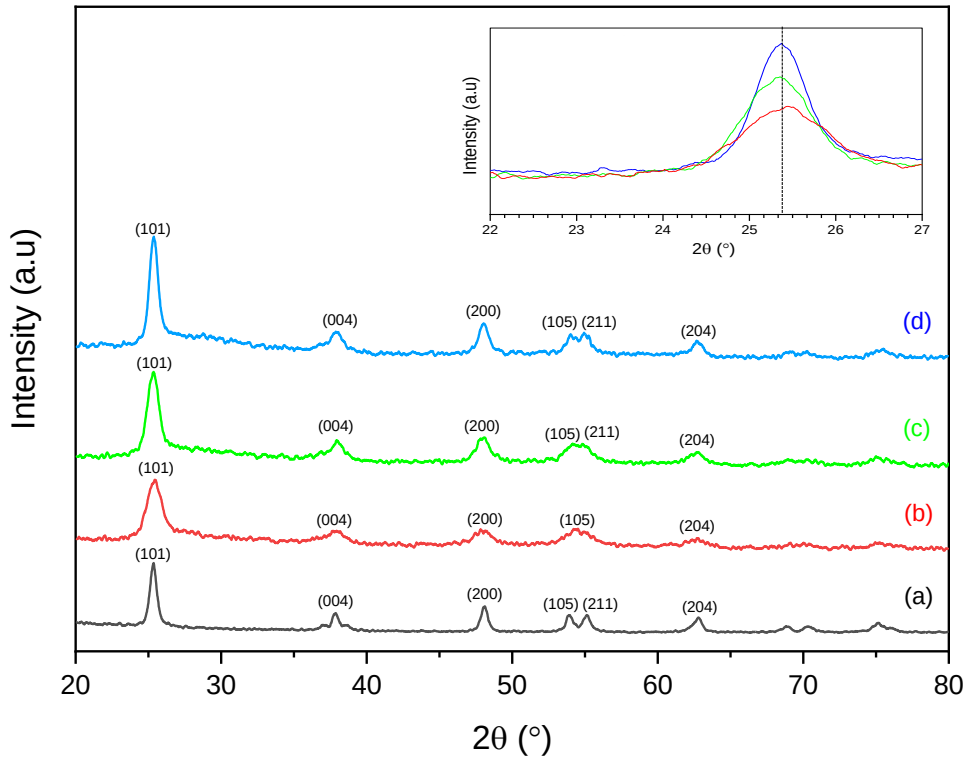

Figure 3. XRD Patterns of (**a**) TiO_2, (**b**) Bi-TiO_2 400°C, (**c**) Bi-TiO_2 500°C, and (**d**) Bi-TiO_2 600°C

XRD patterns of Bi-TiO_2 samples also show that there was no interference in the patterns due to Bi doping, such as no other diffraction peaks. This result shows that Bi has been successfully doped into a TiO_2 structure by substituting Ti^{4+} in lattice sites [16]. The absence of other peaks shows that synthesized samples using a simple sol-gel method have

high purity [12, 17]. Pristine TiO_2 and Bi-TiO_2 400°C have different peaks because of their calcination temperature, where calcination temperature affects crystal growth. At Bi-TiO_2 400°C, the crystal growth is improper, as seen from broad peaks and the absence of peak (211) due to the amorphous structure, resulting in a larger crystallite size and a smaller crystallinity index. The result identified that various calcination temperatures (400°C, 500°C, and 600°C) were still in the anatase phase. The anatase phase shows better photocatalytic activity than the rutile and brookite phases because it produces a larger surface area (smaller particles and crystal size) and slower recombination of electron-hole pairs [15].

XRD analysis is used to determine crystallite size (D) [18] and crystallinity index (CI) [19]. D was calculated using the Debye-Scherrer formula (Equation 2), and CI was calculated using the deconvolution method (Equation 3).

$$D = \frac{K\lambda}{\beta \cos\theta} \quad (2)$$

$$CI\ (\%) = \frac{\text{area of each crystalline peak}}{\text{total area}} \times 100 \quad (3)$$

where D is the size of crystallite, K is the dimensionless shape factor (0.89), λ is the wavelength of Cu Kα radiation (1.5406 Å), β is the full width at half maximum (radian), and θ is the angle of diffraction peak [20]. The average D and CI at various calcination temperatures are shown in Table 1. At low calcination temperatures (400°C), broad peaks are observed due to the amorphous structure of TiO_2. D increased at a high calcination temperature (600oC), whereas CI decreased because its calcination temperature affected crystal growth. The higher the calcination temperature is, the faster crystal growth goes. It was attributed due to the agglomeration with enhancement in calcination temperature that affected the crystallite size. Thus, the CI of 600°C is larger than 500°C, and the CI of 600°C is smaller than 500°C. Crystallite size increases with enhancement in calcination temperature, and the CI will decrease, as seen from the results in Table 1 [21].

Based on Table 1. the smallest D dan largest CI were obtained at 500°C, 11.95 nm and 62.04%. The smaller the crystallite size, the larger the surface area obtained, and the photocatalytic activity will increase [14, 15]. A smaller D is preferred due to its relationship with the surface area when applying photocatalytic materials. Additionally, higher CI is preferred due to its rigidity and highly ordered crystal structure.

Table 1. The Comparison of D and CI Values from TiO_2 and Bi-TiO_2

Sample	Temperature (°C)	D (nm)	CI (%)
TiO_2	450	33.15	50.01
Bi-TiO_2	400	50.92	42.23
	500	11.95	62.04
	600	16.51	61.36

DRS UV-Vis characterization investigates synthesised samples' band gap (Eg) value. Moreover, this characterization shows whether Bi as a dopant succeeds or fails in reducing the Eg of TiO_2 due to the substitution of Bi^{3+} cations into the TiO_2 crystal lattice. Bi, as a dopant, can form impurity levels between valence and conduction bands, causing crystal defects to extend the spectra range to visible light irradiation (red-shift). These crystal defects cause a decrease in Eg value as the concentration of Bi increases. It means that the dopants can absorb visible light. The DRS UV-Vis spectra of TiO_2 and Bi-

TiO_2 at various concentrations are shown in Figure 4. Based on Figure 4, it can be seen that a red shift appeared in the absorption spectra of Bi-TiO_2 compared to TiO_2. This is because the dopants can absorb visible light ranging from 400 to 800 nm [12, 20]. This red shift indicates the modification of the Eg value, which was calculated using the Kubelka-Munk function and Tauc plot [20]. From the spectra, Bi-TiO_2, with the biggest amount of 1.5%, has the highest light absorption, with an estimated λ of 782.33 nm.

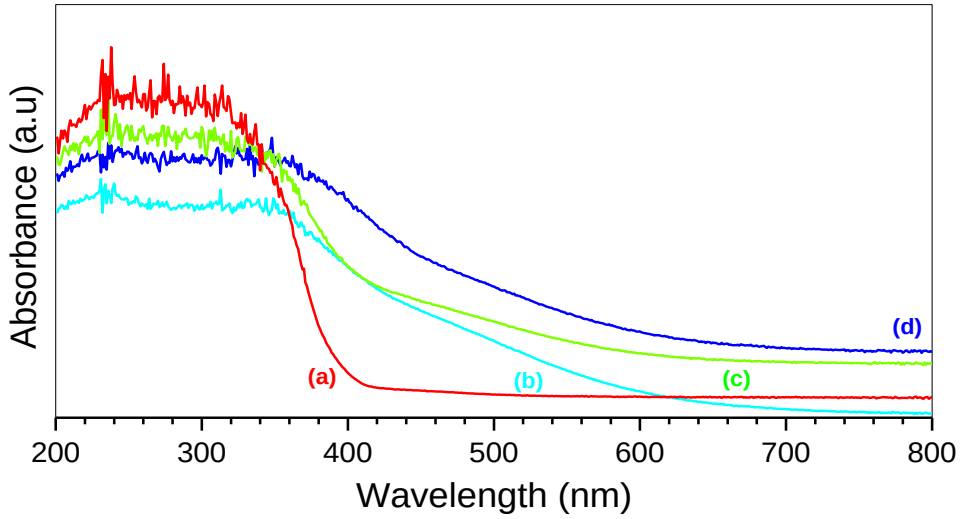

Figure 4. DRS UV-Vis Spectra of (**a**) TiO_2, (**b**) Bi-TiO_2 1%, (**c**) Bi-TiO_2 0.5%, and (**d**) Bi-TiO_2 1.5%

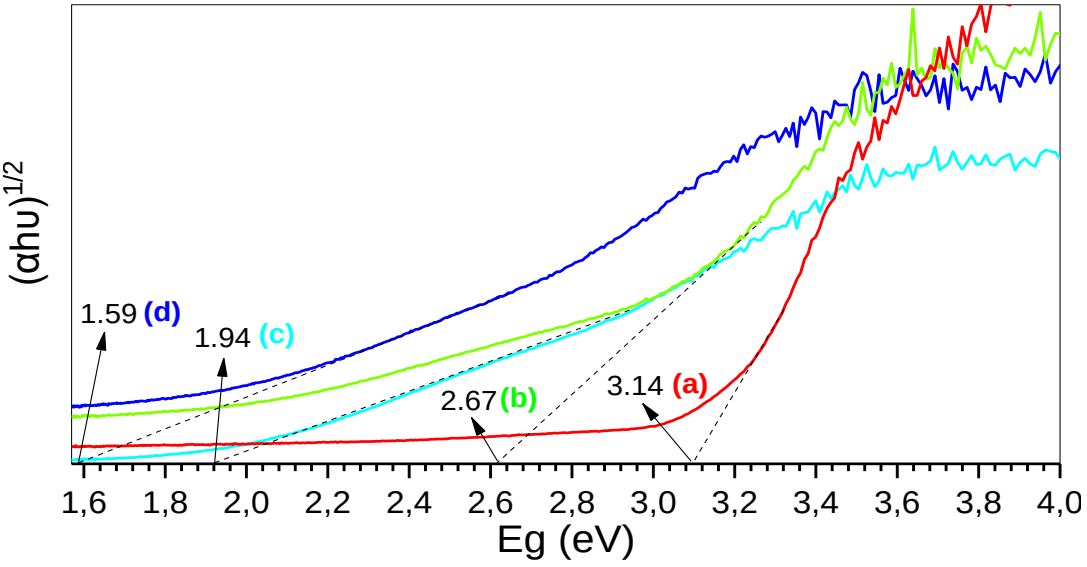

Figure 5. Relation Between Kubelka-Munk Function and Tauc Plot Toward Eg Values of (**a**) TiO_2, (**b**) Bi-TiO_2 0.5%, (**c**) Bi-TiO_2 1%, and (**d**) Bi-TiO_2 1.5%

The Eg value of TiO_2 and Bi-TiO_2 was measured by plotting $(\alpha hu)^{1/2}$ against Eg as a Kubelka-Munk function and extrapolating the linear portion of the curve as a Tauc plot [22]. The relationship between the Kubelka-Munk function and the Tauc plot and the obtained Eg values is shown in Figure 5 and Table 2.

Tabel 2. Eg Values and Wavelength Estimation of Samples

Sample	Eg (eV)	Wavelength (nm)
TiO_2	3.14	395.08
Bi-TiO_2 0.5%	2.67	465.35
Bi-TiO_2 1%	1.94	640.13
Bi-TiO_2 1.5%	1.59	782.33

The results show that Eg value decreased with increasing Bi concentration, from 3.14 eV to 1.59 eV. The reducing Eg value of pristine TiO_2 after being modified by Bi showed the substitution of Bi^{3+} cations into the TiO_2 crystal lattice. This is also supported by the expansion of the Bi-TiO_2 spectra into the visible region due to the modification by Bi. Bi-TiO_2 1.5% yielded the lowest Eg value of 1.59 eV. The smaller the Eg value, the wider the absorption region will extend to the visible light region, allowing it to become more active and absorb visible light.FT-IR characterization was carried out to determine bonds and functional groups in the sample. Furthermore, FT-IR is used to detect the presence of –OH groups adsorbed on the surface of the photocatalyst. –OH groups on the surface produce •OH through reactions with hole (h^+), which play a role in the degradation process of HA [23]. FT-IR characterization was carried out in the wave-number range of 4000-400 cm^{-1}. The obtained FT-IR spectra is shown in Figure 6.

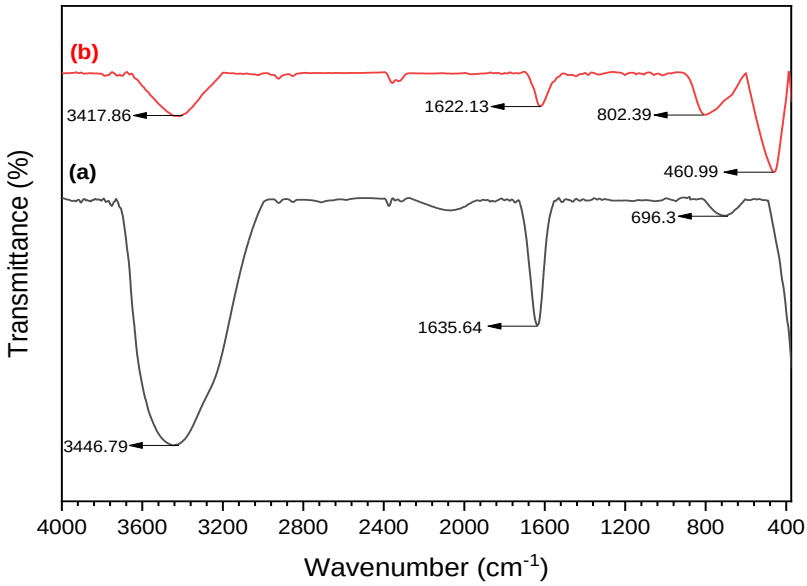

Figure 6. FT-IR Spectra of (**a**) TiO_2 and (**b**) Bi-TiO_2

Based on Figure 6, a bond was observed at 460.99 cm-1 by the stretching vibrations of the Ti-O-Ti bond. [24] has reported that stretching vibrations of the Ti-O-Ti bond were observed at 480.55 cm^{-1}. The absorption band at 802.39 cm^{-1} corresponded to stretching vibrations of the Bi-O bond. Sirimahasal et al. (2017) [25] has reported bond observed at 800 cm^{-1} for stretching vibrations of Bi-O bond. The bond observed at 1622.13 cm^{-1} corresponded to bending vibrations of the adsorbed –OH groups bonding to Ti. This result was related to the research by [26], that the bond appeared at 1623 cm^{-1}. Meanwhile, the bond at 3147.86 cm^{-1} corresponded to stretching

vibrations of the –OH bond from adsorbed water molecules. This bond has similar results to the research by [27], showing a bond appeared at 3147.8 cm^{-1}.

FT-IR results show the redshift due to the formation of the Bi-O bond. The shift occurred due to the substitution of Ti^{4+} with Bi^{3+} cations. Following the addition of Bi, the absorption band of Ti-O-Ti shifted from 696.3 cm^{-1} to 460.99 cm^{-1}. The shift that occurred was caused by forming the Bi-O bond at 802.39 cm^{-1}. The shift toward a smaller wavenumber indicates that light absorption extends to a higher wavelength, as obtained by DRS UV-Vis spectra [28].

Photocatalytic Activity of Bi-TiO_2 for Humic Acid Degradation

The photocatalytic activity of the as-synthesized Bi-TiO_2 was investigated by degrading HA. HA degradation was carried out in a photocatalytic reactor for 180 minutes using as-synthesized pristine TiO_2 and Bi-TiO_2 at various concentrations (0.5%, 1%, and 1.5%) under visible light as a function of irradiation time [20]. The photocatalytic activity was carried out at various Bi concentrations with a calcination temperature of 500°C, the optimum temperature with the highest CI and smaller D. The absorbance was measured using a UV-Vis spectrophotometer at 254 nm [29]. HA degradation percentages is shown in Figure 7.

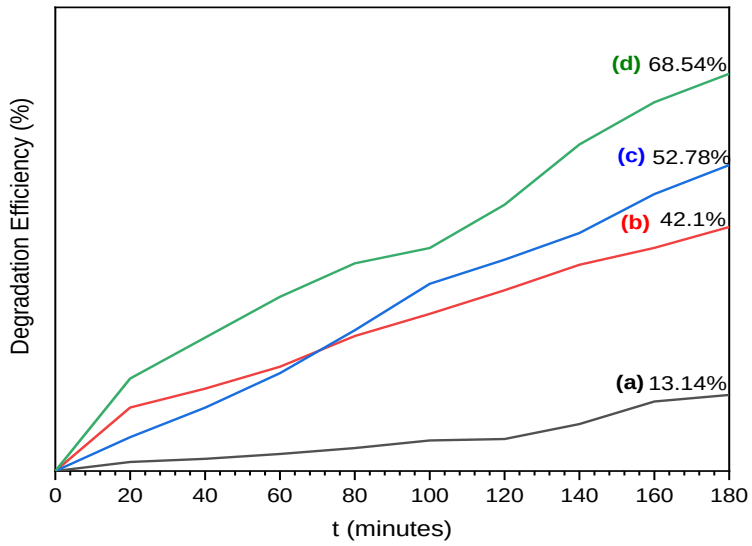

Figure 7. Humic Acid Degradation Efficiency of (**a**) TiO_2, (**b**) Bi-TiO_2 0.5%, (**c**) Bi-TiO_2 1%, and (**d**) Bi-TiO_2 1.5%

HA with the highest to lowest degradation was obtained from Bi-TiO_2 1.5%; 1%; 0.5%; and pristine TiO_2 samples, respectively. As-synthesized pristine TiO_2 has the lowest degradation percentage due to its Eg value, which is in the absorption region of UV light. On the contrary, bi-TiO_2 1.5% has the highest degradation percentage due to its Eg value (1.59 eV). This is due to the enhancement of the absorption region to visible light. Furthermore, the doping process prevented the recombination of electron-hole pairs, which enhanced the photocatalytic activity in the degradation of HA [30].

HA degradation occurs due to the interaction between catalyst and photon on the

surface of TiO_2. When TiO_2 is exposed to photons from visible light irradiation, an electron (e^-) transfer from the valence band (V_B) to the conduction band (C_B) (excitation state) will occur. Hole (h^+) formed at V_B and will react with H_2O or hydroxide ion (OH^-), generating the formation of $^{\bullet}OH$. Meanwhile, e^- on C_B will react with O_2 generating superoxide radical formation ($^{\bullet}O_2^-$). Bi on TiO_2 has a role as an electron-hole trap, hence inhibiting the recombination of electron-hole pairs. The obtained $^{\bullet}OH$ and $^{\bullet}O_2^-$ play a role in degrading organic pollutants such as HA. $^{\bullet}OH$ and $^{\bullet}O_2^-$ are two main active radicals for organic matter elimination [31]. Based on Figure 5, it can be seen that the higher the dopant concentrations are, the higher the degradation percentage of HA obtained. With increasing Bi attention, the formation of $^{\bullet}OH$ and $^{\bullet}O_2^-$ on the surface of TiO_2 will increase due to further penetration of light through the solution, increasing the degradation percentage [32]. At Bi-TiO_2 1.5%, more Bi was used to trap electron and hole, inhibiting electron-hole pairs' recombination to further obtain $^{\bullet}OH$ and $^{\bullet}O_2^-$. The obtained $^{\bullet}OH$ and $^{\bullet}O_2^-$ will degrade HA on the surface of the photocatalyst [33]. The proposed mechanism for HA degradation is represented in Equation (4-8) below [30].

$$\text{Bi/TiO}_2 + h\nu \rightarrow \text{TiO}_2\,(e^-) + \text{bismuth}\,(h^+) \quad (4)$$

$$h^+ + H_2O \rightarrow {}^{\bullet}OH + H^+ \quad (5)$$

$$h^+ + OH^- \rightarrow {}^{\bullet}OH \quad (6)$$

$$e^- + O_2 \rightarrow {}^{\bullet}O_2^- \quad (7)$$

$$h^+ \text{ or } {}^{\bullet}OH \text{ or } {}^{\bullet}O_2^- + \text{humic acid} \rightarrow \text{degraded products} \quad (8)$$

CONCLUSION

In summary, Bi-TiO_2 photocatalysts were successfully synthesized by the sol-gel method. Bi-TiO_2 has become an economical and environmentally friendly method for degrading HA, as it utilizes visible light in the degradation process. Additionally, the photocatalytic method offers advantages over other conventional methods by producing $^{\bullet}OH$ and $^{\bullet}O_2^-$ that break down HA into degradation products like CO_2 and H_2O, resulting in total mineralization. The Eg value of TiO_2 dan Bi-TiO_2 decreased from 3.14 to 1.59 eV by increasing the amount of Bi (0.5% to 1.5%). It is identified that photocatalyst samples are active under visible light irradiation. However, the use of light in this study is a limitation due to its dependence on the photon energy that can be absorbed. Therefore, in future research, the use of sunlight as a light source could be investigated. Additionally, future research could evaluate the use of Bi-TiO_2 composite materials with other materials as a photocatalyst for the degradation of humic acid, as this study only compared Bi-TiO_2 to TiO_2. Calcination under the temperature of 500^{o}C results in the smallest crystallite size dan largest crystallinity index (11.95 nm and 62.04%, respectively). HA degradation reached 68.54% for 180 minutes of irradiation at the as-synthesized Bi-TiO_2 of 1.5%. This indicates that Bi-TiO_2 can be considered for use in larger-scale applications that utilize sunlight to degrade humic acid. This can optimize the photon energy from sunlight as a light source, increasing photocatalytic activity. Based on these findings, it can be concluded that Bi-TiO_2 has the potential to serve as an alternative method for humic acid treatment in peat water.

ACKNOWLEDGEMENT

Thank you to the Dean of FMIPA Tanjungpura University for the submission and author fee assistance.

REFERENCES

[1] N. Chaukura W. Moyo, B. B. Mamba, and T. I. Nkambules, "Abatement of humic acid from aqueous solution using a carbonaceous conjugated microporous polymer derived from waste polystyrene", *Environ. Sci. Pollut. Res.*, vol. 25, pp. 3291-3300, 2018, doi: 10.1007/s11356-017-0691-x

[2] F. Tahmasebi, M. Alimohammadi, R. Nabizadeh, M. Khoobi, K. Karimian, and A. Zarei, "Performance evaluation of graphene oxide coated on cotton fibers in removal of humic acid from aquatic solutions", *Korean J. Chem. Eng.*, vol. 36, pp. 894-902, 2019, doi: 10.1007/s11814-019-0277-z

[3] S. Li, M. He, Z. Li, D. Li, and Z. Pan, "Removal of humic acid from aqueous solution by magnetic multi-walled carbon nanotubes decorated with calcium", *J. Mol. Liq.*, vol. 230, pp. 520-528, 2017, doi: 10.1016/j.molliq.2017.01.027

[4] A. A. Mohammadi, M. H. Dehghani, A. Mesdaghinia, K. Yaghmaian, and Z. Es'haghi, "Adsorptive removal of endocrine disrupting compounds from aqueous solutions using magnetic multi-wall carbon nanotubes modified with chitosan biopolymer based on response surface methodology: Functionalization, kinetics, and isotherms studies", *Int. J. Biol. Macromol.*, vol. 155, pp. 1019-1029, 2020, doi: 10.1016/j.ijbiomac.2019.11.065

[5] T. X. Tung, D. Xu, Y. Zhang, Q. Zhou, and Z. Wu, "Removing Humic Acid from Aqueous Solution Using Titanium Dioxide: A Review", *Pol. J. Environ. Stud*, vol. 28, no. 2, pp. 529-542, 2019, doi: 10.15244/pjoes/85196

[6] F. Scarpelli, T. F. Mastropietro, T. Poerio, and N. Godbert, "Mesoporous TiO_2 Thin Films: State of the Art", *Titanium Dioxide – Material for a Sustainable Environment*, 2018, doi: 10.5772/intechopen.74244

[7] J. L. Song, H. J. Ma, H. Jia, r. F. Wang, and Z. P. Dong, "Facile Synthesis of Amorphous Bi-Doped TiO_2 and Its Visible Light Photocatalytical Properties", *J. Nanosci. Nanotechnol.*, vol. 17, no. 8, pp. 5318-5326, 2017, doi: 10.1166/jnn.2017.13806

[8] A. Alzamly, F. Hamed, T. Ramachandran, M. Bakiro, A. H. Ahmed, S. Mansour, A. Salem, K. A. al, N. S. A. Kaabi, M. Meetani, and A. Khaleel, "Tunable band gap of Bi^{3+}-doped anatase TiO_2 for enhanced photocatalytic removal of acetaminophen under UV-visible light irradiation", *Journal of Water Reuse and Desalination*, vol. 9, no. 1, pp. 31-46, 2018, doi: 10.2166/wrd.2018.021

[9] D. Fatmawati, A. B. Aritonang, and Nurlina, "Sintesis dan Karakterisasi TiO_2-Kaolin Menggunakan Metode Sol Gel", *JKK*, vol. 8, no. 2, pp. 15-21, 2019.

[10] P.A.K. Reddy, B. Srinivas, P. Kala, V. D. Kumari, M. Subrahmanyam, "Preparation and characterization of Bi-doped TiO_2 and its solar photocatalytic activity for the degradation of isoproturon herbicide", *Mater. Res. Bul.l*, vol. 46, no. 11, pp. 1766-1771, 2011, doi: 10.1016/j.materresbull.2011.08.006

[11] S. S. Mohtar, F. Aziz, A. R. M. Nor, A. M. Mohammed, A. A. Mhamad, J. Jaafar, N. Yusof, W. N. W. Salleh, and A. F. Ismail, "Photocatalytic degradation of humic acid using a novel visible-light active α-Fe_2O_3/NiS_2 composite photocatalyst", *J.*

Environ. Chem. Eng., vol. 9, no. 4, 105682, pp. 1-12, 2021, doi: 10.1016/j.jece.2021.105682

[12] D. Liu, C. Li, C. Zhao, E. Nie, J. Wang, J. Zhou, and Q. Zhao, "Efficient Dye Contaminant Elimination and Simultaneously Electricity Production via a Bi-Doped TiO_2 Photocatalytic Fuel Cell", *Nanomaterials*, vol. 12, no. 2, 210, pp. 1-12, 2022, doi: 10.3390/nano12020210

[13] B. Choudhury and A. Choudhury, "Local structure modification and phase transformation of TiO_2 nanoparticles initiated by oxygen defects, grain size, and annealing temperature", *Int. Nano. Lett.*, vol. 3, no. 55, pp. 1-9, 2013, doi: 10.1186/2228-5326-3-55

[14] M. G. Kim, J. M. Kang, J. E. Lee, K. S. Kim, K. H. Kim, M. Cho, and S. G. Lee, "Effects of Calcination Temperature on the Phase Composition, Photocatalytic Degradation, and Virucidal Activities of TiO_2 Nanoparticles", *ACS Omega*, vol. 6, no. 16, pp. 10668-10678, 2021, doi: 10.1021/acsomega.1c00043

[15] N. K. Reddy, G. K. Reddy, K. M. Basha, P. K. Mounika, and M. V. Shankar, "Highly Efficient Hydrogen Production using Bi_2O_3/TiO_2 Nanostructured Photocatalysts Under Led Light Irradiation", *Mater. Today Proc.*, vol. 3, no. 6, pp. 1351-1358, 2016, doi: 10.1016/j.matpr.2016.04.014

[16] A. Charanpahari, S. C. Ghugal, S. S. Umare, and R. Sasikala, "Mineralization of malachite green dye over visible light responsive bismuth doped TiO_2-ZrO_2 ferromagnetic nanocomposites", *New J. Chem.*, vol. 39, no. 5, pp. 3629-3638, 2015, doi: 10.1039/C4NJ01618A

[17] H. Xiang, B. Tuo, J. Tian, K. Hu, J. Wang, J. Cheng, and Y. Tang, "Preparation and photocatalytic properties of Bi-doped TiO_2/montmorillonite composite", *Opt. Mater. (Amst)*, vol. 117, no. 111137, pp. 1-8, 2021, doi: 10.1016/j.optmat.2021.111137

[18] Y. Ma, X. Yang, G. Gao, Z. Yan, H. Su, B. Zhang, Y. Lei, and Y. Zhang, "Photocatalytic partial oxidation of methanol to methyl formate under visible light irradiation on Bi-doped TiO_2 *via* tuning band structure and surface hydroxyls", *RSC Adv.*, vol. 10, no. 52, pp. 31442-31452, 2020, doi: 10.1039/D0RA06309F

[19] M. Ferro, A. Mannu, W. Panzeri, C. H. J. Theeuwen, and A. Mele, "An Integrated Approach to Optimizing Cellulose Mercerization", *Polymers*, vol. 12, no. 7, 1559, pp. 1-16, 2020, doi: 10.3390/polym12071559

[20] S. Estrada-Flores, C. M. Pérez-Berumen, T. E. Flores-Guia, L. A. García-Cerda, J. Rodríguez-Hernández, T. A. Esquivel-Castro, and A. Martínez-Luévanos, "Mechanosynthesis of Mesoporous Bi-Doped TiO_2: The Effect of Bismuth Doping and Ball Milling on the Crystal Structure, Optical Properties, and Photocatalytic Activity", *Crystals*, vol. 12, no. 1750, pp. 1-18, 2022, doi: 10.3390/cryst12121750

[21] M. Lal, P. Sharma, and C. Ram, "Calcination Temperature Effect on Titanium Oxide (TiO_2) Nanoparticles Synthesis", *Optik*, vol. 241. no. 166934, pp. 1-26, 2021, doi: 10.1016/j.ijleo.2021.166934

[22] G. Nagaraj, A. D. Raj, A. A. Irudayaraj, R. L. Josephine, "Tuning the optical band Gap of pure TiO_2 via photon induced method", *Optik*, vol. 179, no. 1, pp. 889-894, 2018, doi: 10.1016/j.ijleo.2018.11.009

[23] Ü. Ünlü, S. Kemeç, and G. S. P. Soylu, "The impact of alkaline earth oxides on Bi_2O_3 and their catalytic activities in photodegradation of Bisphenol A", *Turk.*

J. Chem., vol. 45, no. 3, pp. 683-693, 2021, doi: 10.3906%2Fkim-2101-30

[24] K. M. Prabu and P. M. Anbarasan, "Preparation and Characterization of Silver, Magnesium & Bismuth Doped Titanium Dioxide Nanoparticles for Solar Cell Applications", *IJSR*, vol. 3, no. 9, pp. 132-137, 2014.

[25] T. Sirimahasal, S. Pranee, S. Chuayprakong, S. Durmus, and S. Seeyangnok, "Synthesis and Characterization of Bismuth Oxo Compounds Supported on TiO_2 Photocatalysts for Waste Water Treatment", *Key Eng. Mater.*, vol. 757, pp. 108-112, 2017, doi:10.4028/www.scientific.net/KEM.757.108

[26] W. Wang, D. Zhu, Z. Shen, J. Peng, J. Luo, and X. Liu, "One-Pot Hydrothermal Route to Synthesize the Bi-doped Anatase TiO_2 Hollow Thin Sheets with Prior Facet Exposed for Enhanced Visible-Light-Driven Photocatalytic Activity", *Ind. Eng. Chem. Res*, vol. 55, 22, pp. 6373-6383, 2016, doi: 10.1021/acs.iecr.6b00618

[27] S. Bagwasi, Y. Niu, M. Nasir, B. Tian, and J. Zhang, "The study of visible light active bismuth modified nitrogen doped titanium dioxide photocatalysts: Role of bismuth", *Appl. Surf. Sci.*, vol. 264, pp. 139-147, 2013, doi: 10.1016/j.apsusc.2012.09.145

[28] A. B. Aritonang, E. Pratiwi, W. Warsidah, S. I. Nurdiansyah, and R. Risko, "Fe-doped TiO_2/Kaolinite as an Antibacterial Photocatalyst under Visible Light Irradiation", *BCRC*, vol. 16, no. 2, pp. 293-301, 2021, doi: 10.9767/bcrec.16.2.10325.293-301

[29] S. M. Pormazar, M. H. Ehrampoush, and A. Dalvand, "Removal of Humic Acid from Aqueous Solution by Fe_3O_4@L-Arginine Magnetic Nanoparticle: Kinetic and Equilibrium Studies", *Int. J. Environ. Anal. Chem.*, vol. 102, no. 14, pp. 1-6, 2020, doi: 10.1080/03067319.2020.1767092

[30] I. Ali, S. R. Kim, S. P. Kim, and J. O. Kim, "Anodization of bismuth doped TiO_2 nanotubes composite for photocatalytic degradation of phenol in visible light", *Catal. Today*, vol. 282, no. 1, pp. 31-37, 2017, doi: 10.1016/j.cattod.2016.03.029

[31] J. S. Barroso-Martínez, S. I. B. Romo, S. Pudar, S. T. Putnam, E. Bustos, and J. Rodríguez-López,, "Real-Time Detection of Hydroxyl Radicals Generated at Operating Electrodes via Redox-Active Adduct Formation Using Scanning Electrochemical Microscopy", *J. Am. Chem. Soc*, vol. 144, no. 41, pp. 18896-18907, 2022, doi: 10.1021/jacs.2c06278

[32] S. G. Shelar, V. K. Mahajan, S. P. Patil, and G. H. Sonowane, "Effect of doping parameters on photocatalytic degradation of methylene blue using Ag doped ZnO nanocatalyst", *SN Appl. Sci.*, vol. 2, no. 802, pp. 1-10, 2020, doi: 10.1007/s42452-020-2634-2

[33] A. Abdelhaleem and W. Chu, "Prediction of Carbofuran Degradation Based on the Hydroxyl Radical's Generation using the Fe^{III} impregnated N doped-TiO_2/H_2O_2/Visible LED Photo-Fenton-like Process", *Chemical Engineering Journal*, vol. 382, no. 122930, pp. 1-40, doi: 10.1016/j.cej.2019.122930